Time Dependence of Resonantly Filtered Gamma Rays from Fe^{57}†

F. J. Lynch, R. E. Holland, and M. Hamermesh
Argonne National Laboratory, Argonne, Illinois

(Received June 6, 1960)

The time dependence of gamma rays emitted by the 14.4-kev state of Fe^{57} has been studied by delayed-coincidence measurements between a 123-kev gamma ray preceding formation of the state and the 14.4-kev gamma ray from the state. When no filter was used, the number of gamma rays decreased exponentially with the known half-life of 0.1 μsec. When a foil of Fe^{57} (which was resonant to 14.4-kev radiation) was used as a filter, the number of gamma rays observed through the filter did not decrease exponentially. Instead, the filter absorbed almost none of the gamma rays first emitted by the 14.4-kev state; at later times the absorption increased. Data were taken with three different thicknesses of absorber and with emission and absorption peaks separated by 0 to 11 times the width of the resonance. The energy separation resulted from the Doppler shift associated with a constant velocity between source and absorber. These data were, for the most part, in good accord with the prediction of a theory based on a classical model for absorber and source. In particular, the results verified the theoretical prediction that at certain times the intensity of radiation observed would be greater with the filter than without it.

I. INTRODUCTION

IN an earlier paper,[1] we showed that the intensity of the gamma rays transmitted through an absorber which is resonant to the incident gamma radiation does not decrease exponentially with time. Instead, the transmitted beam appears initially to decay faster than the rate corresponding to the life-time τ of the emitting state. The intuitive picture which led us to undertake the initial experiments was that the resonance absorption tends to reduce the intensity at the center of the emitted line relative to the intensity in the wings. Thus the width at half maximum of the remaining peak is greater than the value $\Gamma=\hbar/\tau$ of the original peak; and the lifetime of the state appears to be correspondingly shorter.

A quantitative theoretical treatment was developed by describing the emitted radiation as a damped electromagnetic wave.[2] On passing through a medium filled with resonators, the frequency spectrum of the radiation is altered, so that its time dependence is no longer exponential. The theoretical analysis, which is presented in Sec. II, suggested some of the experiments which are described in Sec. III.

The 14.4-kev state of Fe^{57} provides a convenient source for observation of this effect. The formation of the 14.4-kev state is announced by a 123-kev gamma ray in the decay[3] of Co^{57}, the Mössbauer effect is large[4] (about 60% of the radiation is emitted without recoil at room temperature), the half-life[3] is 0.1 μsec, and the gamma ray is highly converted[5] ($\alpha=15$) so that imprisonment of the resonance radiation need not be considered.

II. THEORY

The time dependence of the 14-kev radiation of Fe^{57} as observed in transmission through an Fe^{57} absorber can be explained on a simple classical theory. As in standard treatments of emission and dispersion, the medium is assumed to consist of damped oscillators with natural frequency ω_0 and decay constant λ. The radiation emitted by the Fe^{57} source has an electric field

$$a(t)=\exp[i\omega_0 t-\tfrac{1}{2}\lambda t]=\frac{1}{2\pi i}\int_{-\infty}^{+\infty}d\omega\frac{e^{i\omega t}}{\omega-\omega_0-\frac{1}{2}i\lambda}$$

$$=\int_{-\infty}^{+\infty}d\omega\, a(\omega)e^{i\omega t}. \quad (1)$$

The constant λ is just the reciprocal of the mean life of the excited state. In the case of the 14-kev line of Fe^{57}, 93% of the radiation is internally converted; the quantity λ contains contributions from all types of decay (radiation and internal conversion).

The effect of transmission through the Fe^{57} absorber can be found by standard methods.[6] Each monochromatic component $a(\omega)e^{i\omega t}$ excites forced oscillations of the resonators in the medium. The complex dielectric constant is

$$\epsilon(\omega)=1+r(\omega_0'^2-\omega^2+i\omega\lambda)^{-1}. \quad (2)$$

We have written ω_0' for the resonant frequency of the absorber to take account of a possible Doppler shift due to motion relative to the source.

† Work performed under the auspices of the U. S. Atomic Energy Commission.

[1] R. E. Holland, F. J. Lynch, G. J. Perlow, and S. S. Hanna, Phys. Rev. Letters 4, 181 (1960).

[2] M. Hamermesh, Argonne National Laboratory Report ANL-6111, February, 1960 (unpublished), p. 6.

[3] *Nuclear Data Sheets*, National Academy of Sciences, National Research Council, 1959 (U. S. Government Printing Office, Washington, D. C.).

[4] R. L. Mössbauer, Z. Physik **151**, 124 (1958); J. P. Schiffer and W. Marshall, Phys. Rev. Letters **3**, 556 (1959); R. V. Pound and J. A. Rebka, Jr., Phys. Rev. Letters **3**, 554 (1959).

[5] H. R. Lemmer, O. J. A. Segaert, and M. A. Grace, Proc. Phys. Soc. (London) **A68**, 701 (1955).

[6] J. A. Stratton, *Electromagnetic Theory* (McGraw-Hill Book Company, Inc., New York, 1941), p. 321.

From Eq. (2), the propagation vector in the medium is found to be

$$k=(\omega/c)[1+\tau(\omega_0'^2-\omega^2+i\omega\lambda)^{-1}]^{\frac{1}{2}}. \quad (3)$$

The wavelength of the radiation is about 10^{-8} cm and, as in the x-ray case, we can expand Eq. (3) and retain only the first term. The effect of passage through the absorber is to change $a(\omega)$ to $a'(\omega)$, where

$$a'(\omega)=a(\omega)\exp\{-2ib\omega[\omega_0'^2-\omega^2+i\omega\lambda]^{-1}\}, \quad (4)$$

in which b is a constant.

At $\omega=\omega_0'$, $a'(\omega_0')=a(\omega_0')\exp[-2b/\lambda]$, so the transmission at the center of the line is $\exp[-4b/\lambda]$.

By combining Eqs. (1) and (4), the time dependence of the transmitted amplitude is found to be

$$a'(t)=\frac{1}{2\pi i}\int_{-\infty}^{+\infty}d\omega\frac{e^{i\omega t}}{\omega-\omega_0-\frac{1}{2}i\lambda}\exp\left[\frac{2ib\omega}{\omega^2-\omega_0'^2-i\omega\lambda}\right]. \quad (5)$$

This integral is evaluated in the Appendix with the result expressed as either

$$a'(t)=\exp[i\omega_0't-\tfrac{1}{2}\lambda t]\times\sum_{n=0}^{\infty}\left[\frac{i\{\omega_0-\omega_0'\}}{b}\right]^n(bt)^{\frac{1}{2}n}J_n(2b^{\frac{1}{2}}t^{\frac{1}{2}}), \quad (6a)$$

or

$$a'(t)=\exp\left[i\omega_0't-\frac{\lambda}{2}t\right]\left\{-\exp i\left[\frac{b}{\omega_0-\omega_0'}+(\omega_0-\omega_0')t\right]+\sum_{n=1}^{\infty}\left(\frac{ib}{\omega_0-\omega_0'}\right)^n(bt)^{-n/2}J_n(2b^{\frac{1}{2}}t^{\frac{1}{2}})\right\}. \quad (6b)$$

The time dependence of the transmitted intensity is given by $|a'(t)|^2$. Setting $\omega_0-\omega_0'=\Delta\omega$, $\beta=4b/\lambda$, and

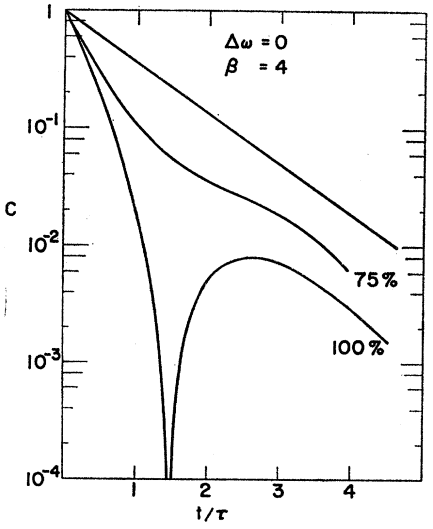

FIG. 1. Time dependence of radiation after transmission through a resonant filter according to Eq. (7), assuming all radiation is recoilless or 75% is recoilless ($\beta=4$, $\Delta\omega=0$). The straight line represents an exponential decay for comparison.

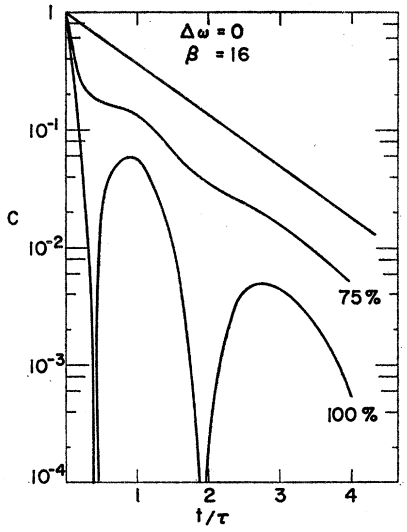

FIG. 2. Time dependence of radiation after transmission through a resonant filter according to Eq. (7), assuming all radiation is recoilless or 75% is recoilless ($\beta=16$, $\Delta\omega=0$). The straight line represents an exponential decay for comparison.

$T=\lambda t$ in Eq. (6a) yields

$$|a'(T)|^2=e^{-T}\left|\sum_{n=0}^{\infty}\left[\frac{4}{i\beta}\frac{\Delta\omega}{\lambda}\right]^n\left[\frac{\beta T}{4}\right]^{\frac{1}{2}n}J_n(\beta^{\frac{1}{2}}T^{\frac{1}{2}})\right|^2. \quad (7)$$

In particular, for $\Delta\omega=0$ this reduces to

$$|a'(T)|^2=e^{-T}[J_0(\beta^{\frac{1}{2}}T^{\frac{1}{2}})]^2. \quad (6)$$

For large values of $\Delta\omega$, the series (7) converges very slowly. In this region, we use Eq. (6b) for $a'(t)$. The transmitted intensity is

$$|a'(T)|^2=e^{-T}\left|-\exp i\left[\frac{\Delta\omega}{\lambda}T+\frac{\lambda}{\Delta\omega}\frac{\beta}{4}\right]+\sum_{n=1}^{\infty}\left[\frac{\beta}{i4}\frac{\lambda}{\Delta\omega}\right]^n\left[\frac{\beta T}{4}\right]^{-\frac{1}{2}n}J_n(\beta^{\frac{1}{2}}T^{\frac{1}{2}})\right|^2. \quad (9)$$

In computing the time behavior of the transmitted intensity, Eq. (7) converges rapidly for

$$\frac{2}{\beta}\frac{\Delta\omega}{\lambda}(\beta T)^{\frac{1}{2}}<1,$$

while Eq. (9) gives rapid convergence for

$$\frac{2}{\beta}\frac{\Delta\omega}{\lambda}(\beta T)^{\frac{1}{2}}>1.$$

The detailed comparison of the theoretical formulas with the experimental results is quite complicated. Here we only indicate some of the points to be considered.

Only some fraction of the 14-kev radiation is recoil-

less, while the remainder is shifted far from resonance and decays exponentially. In Figs. 1 and 2 we show the time dependence of the transmitted beam for two different absorber thicknesses when $\Delta\omega=0$, for the pure resonance radiation and for the case when 75% of the radiation is recoilless.

The effect of relative motion of source and absorber on the time dependence of the transmitted beam is shown in Fig. 3 ($\Delta\omega=\frac{1}{2}\lambda$) and Fig. 4 ($\Delta\omega=4\lambda$).

Figure 4 shows the surprising behavior which should occur as the source and absorber frequency are separated more and more: the intensity oscillates about the exponential curve. Thus, *at certain times* more gamma rays are received *through* the absorber than would have arrived if the absorber were absent. The medium behaves like a resonant filter and appears to "ring" in response to the incident damped oscillation. As $\Delta\omega$ is increased the oscillations shown in Fig. 4 are shifted toward shorter and shorter times so that, for very large $\Delta\omega$, the normal exponential decay is approached.

The transmitted intensity given by Eq. (7) or (9) can be written as

$$|a'(t)|^2=\exp(-\lambda t)F(\beta,t),$$

where $\lambda=1/\tau$. The deviations from exponential behavior are more easily seen if one plots the product of the counting rate with the factor $\exp(\lambda t)$. For the emitted line this product is a constant. For the transmitted line, the theory predicts that the product will vary as $F(\beta,t)$.

The theory given above assumes that there is a single emission (and absorption) line. However, the 14.4-kev line of Fe^{57} has a hyperfine structure of six lines.[7] Since the separation of the hyperfine components is large compared to the linewidth, we assume that

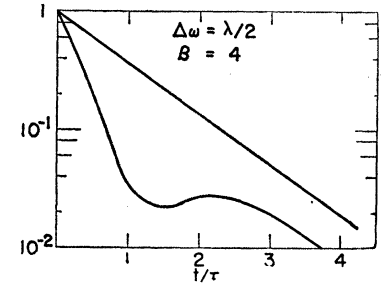

FIG. 3. Effect of relative motion on time dependence of transmitted radiation according to Eq. (7) ($\beta=4$, $\Delta\omega=\frac{1}{2}\lambda$). For comparison, the straight line represents an exponential decay.

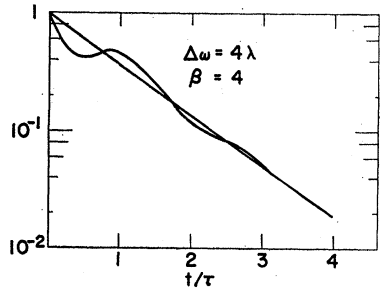

FIG. 4. Effect of relative motion on time dependence of transmitted radiation according to Eq. (7) ($\beta=4$, $\Delta\omega=4\lambda$). For comparison, the straight line represents an exponential decay.

[7] S. S. Hanna, J. Heberle, C. Littlejohn, G. J. Perlow, R. S. Preston, and D. H. Vincent, Phys. Rev. Letters 4, 177 (1960).

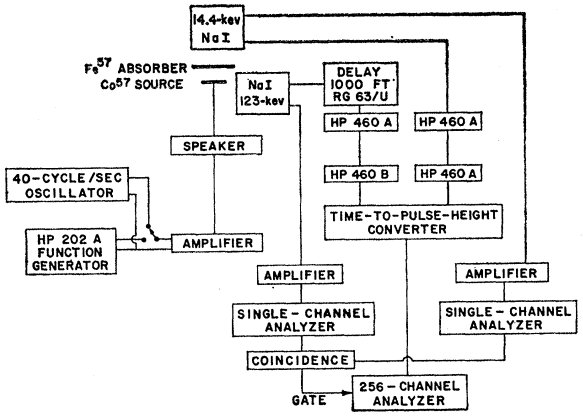

FIG. 5. Schematic diagram of equipment.

each emitted hyperfine component is absorbed only in the corresponding transition in the absorber. By use of the values for the intensities of the hyperfine components, the time dependence of the transmitted radiation is found to be

$$|a'(t)|^2=\exp(-\lambda t)[1-f+f\{\tfrac{1}{2}F(\tfrac{1}{4}\beta,t)+\tfrac{1}{3}F(\tfrac{1}{6}\beta,t)+\tfrac{1}{6}F(\tfrac{1}{12}\beta,t)\}], \quad (10)$$

where f is the fraction of gamma rays emitted without recoil and β is the thickness of the absorber expressed in mean free paths at the peak of the absorption curve. Although in principle β is measurable, it is difficult to determine it accurately. We have used β as a parameter in fitting the theoretical formula to the experimental data. Equation (10) was evaluated on an IBM-704 computer for various values of β and the other parameters, and the calculated curve giving the best visual fit was plotted with the data. One should expect that β would be given by $N\sigma_0 f'$, where f' is the fraction of Fe^{57} nuclei which can absorb without recoil, N is the number of atoms of Fe^{57} per cm^2, $\sigma_0=4\pi\lambda\!\!\!^{-2}/(1+\alpha)$, $\lambda\!\!\!^{-}$ is the wavelength of the 14.4-kev gamma ray divided by 2π, and α is the internal conversion coefficient.

III. EQUIPMENT AND PROCEDURE

The measurements were made with a source of Co^{57} (25 000 disintegrations of Co^{57} per sec) co-plated[8] with Fe^{56} on a thin copper foil and annealed in vacuum at 800°C. Absorbers consisted of rolled foils of Fe^{57} (enriched to 75% in Fe^{57}) or normal Armco iron rolled foils annealed at 800°C. The geometric arrangement of source, absorber, and detectors is shown schematically in Fig. 5. The source, $\frac{3}{8}$ in. in diameter, was mounted on an extension of the speaker diaphragm which could be used to shift the resonant frequency of the source by the Doppler effect. The absorber foil (1 in. in diameter) was clamped between two Lucite disks mounted $\frac{3}{8}$ in. above the source. The detector for the 14.4-kev gamma

[8] S. S. Hanna, J. Heberle, C. Littlejohn, G. J. Perlow, R. S. Preston, and D. H. Vincent, Phys. Rev. Letters 4, 28 (1960).

ray consisted of a NaI(Tl) scintillator 1 in. in diameter and 0.006 in. thick mounted on a Lucite light pipe and an RCA 7265 photomultiplier tube. A second NaI(Tl) scintillator, 1 in. in diameter and $\frac{1}{4}$ in. thick, served as a detector for the 123-kev gamma ray and was mounted $\frac{1}{2}$ in. from the source on a line making an angle of 120° with the line connecting the centers of the other detector and the source.

The speaker coil was driven with a peak-to-peak amplitude of $\frac{1}{8}$ in. by the amplified signal coming alternately from a triangular wave generator[9] and from a 40-cps sinusoidal signal. The triangular wave caused the source to move with a constant velocity either toward or away from the absorber, except during the short interval of reversal of direction. This constant velocity produced a small constant increase or decrese in gamma-ray energy through the Doppler effect. On the other hand, the sinusoidal signal, because of its much higher frequency, produced a wide range of energy shifts; most of the time the gamma rays were not resonant nor even nearly resonant with the absorber. Other sources of absorption, such as the photoelectric effect, would be scarcely affected by the energy shift. Thus we observed the effect of both nonresonant and resonant absorption for small energy shifts with the triangular wave applied to the voice coil and we observed the effect of nonresonant absorption alone with the sinusoidal voltage applied to the voice coil.

Because the average geometric arrangement was slightly different for the two signals, measurements were taken without an absorber, and the sinusoidal signal was adjusted slightly to bring the coincidence counting rate within 1% of the counting rate with the triangular drive.

It is desirable that the triangular wave of voltage should move the source with constant speed. The degree to which this condition holds is determined by the linearity of speaker movement with current, the linearity of the triangular wave voltage, the duration of the transient vibration occurring during reversal of the direction of motion, and the isolation of the system from mechanical vibrations conducted by the air or by the building.

We investigated the movement of the voice coil as a function of current and found the relationship to be linear within the accuracy of measurement (2%). The duration of the transient at the peaks of the triangular wave from the generator was known to be small. From the observed duration of the transient voltage induced by a sudden displacement of the voice coil, the effect due to the inertia of the voice coil and source holder was estimated to be less than 25 msec. At the frequencies we used (<0.2 cps), this corresponded to less than 1% of the period.

The transmission of noise to the speaker was greatly reduced by mounting the assembly consisting of speaker, source, absorber, and detectors in a box lined with sound-absorbing material and acoustically isolated from the floor. With these precautions, the observed vibration of the voice coil because of acoustic noise was less than 0.0004 in. per sec, which should be compared to the velocity of 0.0037 in. per sec needed to produce a Doppler shift of one resonance width. The over-all performance of the system was investigated by observing the width of the central dip in transmission. This was 20% wider than expected for the thickest absorber and 40% wider for the thinnest.

The circuits for measuring the coincidence rate as a function of time delay after formation of the 14.4-kev state are shown schematically in Fig. 5 and were the same (except for slight modifications) as those used previously to measure the lifetimes of excited states of nuclei.[10] The output of the time-to-pulse-height converter was stored in the right half of the 256-channel analyzer when the voice coil was driven with the triangular wave and in the left half when the voice coil was driven with the sinusoidal voltage. During a run, the triangular wave and sinusoidal voltages were applied alternately for 4-min intervals by a timing mechanism, and data were accumulated over a 24-hr period. Signals from slow amplifiers and single-channel analyzers set on the photopeaks of the two gamma rays were required in order to record an event.

Because of the method of recording data, slow drifts were not important. The calibration of the time-to-pulse-height converter (as obtained by using the data from the sinusoidal run to measure the lifetime of the 14.4-kev state of Fe^{57}) remained constant within 1.5% over a period of 1 month. A slow drift of the peak channel was also observed (about $\frac{1}{4}$ channel per day). The converter was linear to within 1% in the region of interest.

IV. RESULTS AND DISCUSSION

The results of a typical measurement for the thickest absorber foil (2.7 mg/cm^2 of Fe^{57}, isotopic enrichment 75%) is shown in Fig. 6. The upper part of the figure shows a conventional semilogarithmic plot of the data after subtraction of background due to accidental coincidences. This background was determined from the counting rate at times preceding the peak shown in Fig. 6(a). In general it was less for the part of the run in which the source was moved at constant velocity than for the part in which the source was vibrated sinusoidally because the counting rate in the 14.4-kev detector was less in the former condition. The total number of accidental coincidences was 2.5% of the total number of true coincidences for the data with vibrated source shown in Fig. 6. The steep rise at the left side of the figure represents the time resolution of the fast circuit; it corresponds to a resolution curve

[9] Model 202A function generator, manufactured by Hewlett-Packard Company, Palo Alto, California.

[10] F. J. Lynch and R. E. Holland, Phys. Rev. **114**, 825 (1959); R. E. Holland and F. J. Lynch, Phys. Rev. **113**, 903 (1959).

with a full width at half maximum of 25 mμsec. The curve obtained with vibrated source shows the exponential decay with a half-life of 0.10 μsec in agreement with previous measurements.[3] The curve obtained with the stationary source demonstrates the effect we expected.

The lower portion of Fig. 6 shows the same data plotted in such a way as to exhibit the deviations from exponential decay predicted in Sec. II. Here the count in each time channel has been multiplied by $e^{\lambda t}$, where λ is the decay constant and t is the time, and the resulting numbers have been adjusted so that the average value of the vibrated data was equal to unity after the initial rise. Data in several adjacent channels were averaged when the counting rate was low. Vertical bars give the standard deviations as calculated from the number of counts. The solid curve shown was calculated for this absorber from the prescription given at the end of Sec. II, with the thickness parameter β adjusted for best fit to the data. This value of β was twice that expected from the thickness of the absorber.

Figure 7 gives typical results for a number of runs in which the source was moved at constant velocity alternately toward and away from the absorber, and data were accumulated without distinguishing the direction of motion. This motion of the source produced

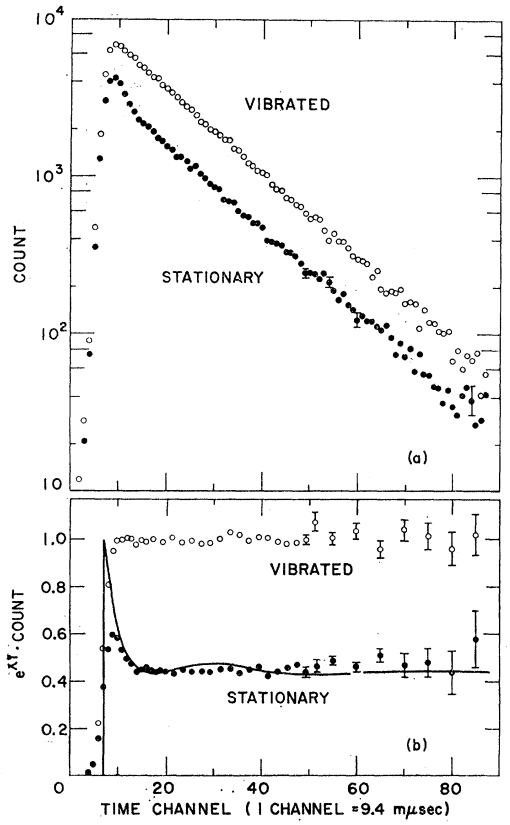

FIG. 6. (a) Semilogarithmic plot of delayed time spectra taken with source and absorber (2.7 mg/cm^2 of Fe^{57}, isotopic abundance 75%) stationary and with source and absorber vibrated relative to one another; (b) Data of Fig. 6(a) replotted with ordinate multiplied by $e^{\lambda t}$ in order to compare with theoretical expression given by the solid line.

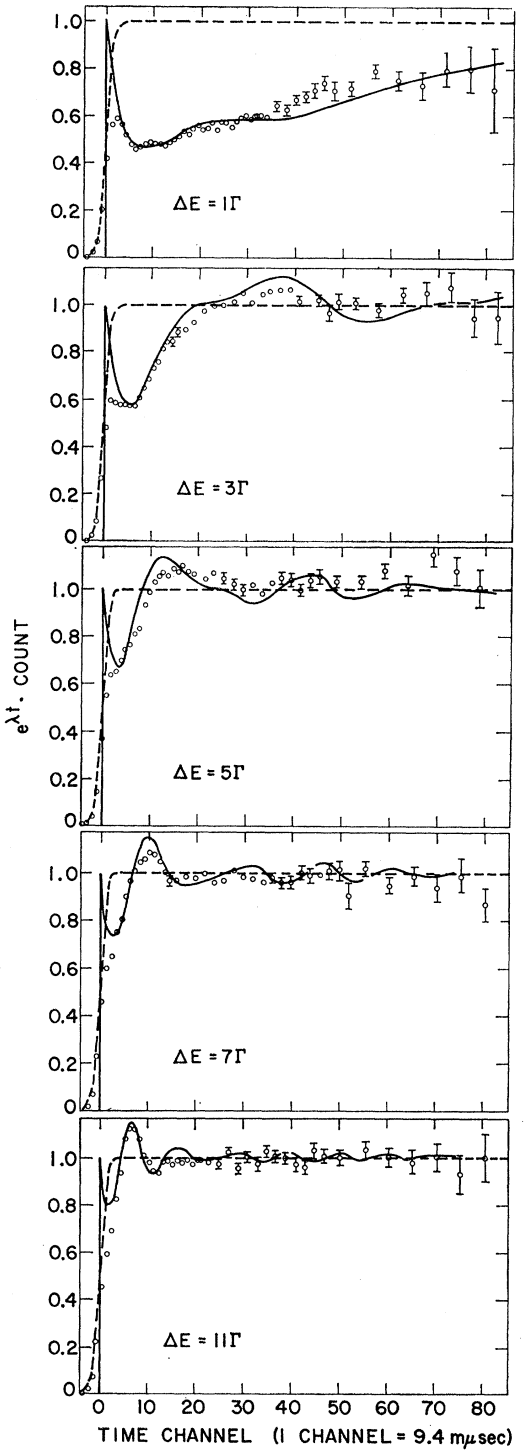

FIG. 7. Time spectra obtained with various energy shifts of the emitted gamma ray. The absorber was the same as in Fig. 6. The energy shift ΔE is given in terms of the linewidth deduced from the mean life of the state, $\Gamma=\hbar/\tau$. The dashed curves give the time spectra when the source is vibrated; the solid curves are the theoretical predictions.

a shift in energy of the emitted gamma ray. The amount of the shift, ΔE, is given on the figure in terms of $\Gamma=\hbar/\tau$, the expected full width at half maximum of the emitted line. The data taken with the source vibrated has been represented in these figures by the light dashed line in order to keep the number of data points from becoming so large as to be confusing. The solid curve is as before a theoretical curve calculated according to Sec. II, with the foil thickness parameter the same as that used in Fig. 2. Similar data for a thinner foil (1.27 mg/cm^2 of Fe^{57} in an enriched foil) is shown in Fig. 8 and for a still thinner foil (0.22 mg/cm^2 of Fe^{57} in a normal isotopic concentration) in Fig. 9.

Not shown are data which were obtained to verify the prediction of the theory that the delayed time spectrum depends only on the magnitude of the shift in gamma-ray energy and not on its sign. A run was made in which data were accumulated only during travel of the source in one direction and the result was compared with that obtained when data were accumulated during travel in both directions. No difference could be observed between the two runs.

All of the data have been compared to the theoretical

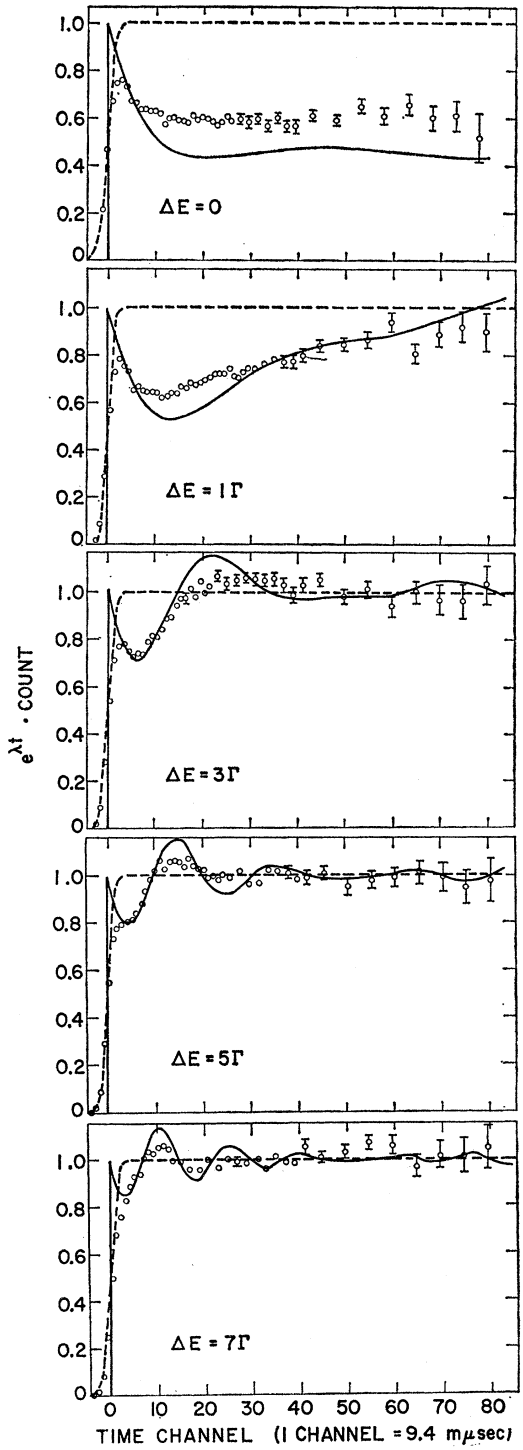

FIG. 8. Time spectra obtained with various energy shifts of the emitted gamma ray. The absorber was a rolled foil (1.27 mg/cm^2 of Fe^{57}, isotopic abundance 75%). The energy shift ΔE is given in terms of the line width deduced from the mean life of the state, $\Gamma=\hbar/\tau$. The dashed curves give the time spectra when the source was vibrated; the solid curves are the theoretical predictions.

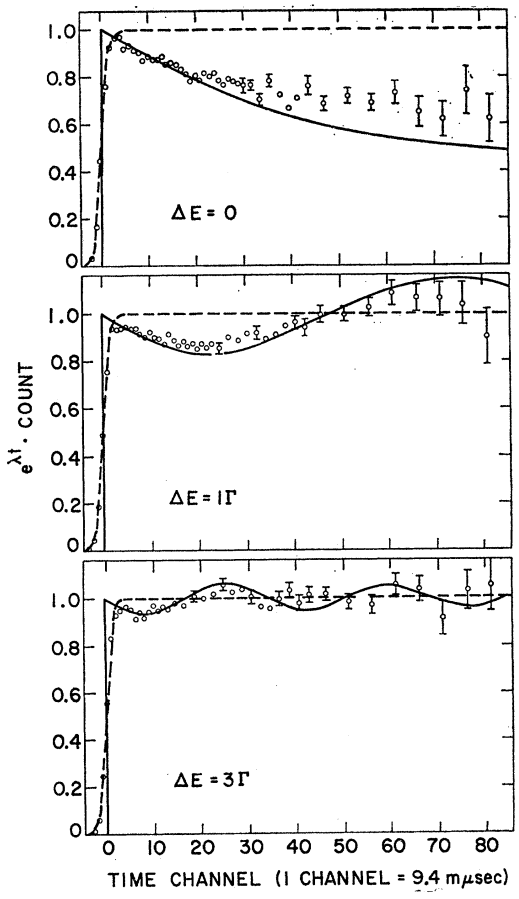

FIG. 9. Time spectra obtained with various energy shifts of the emitted gamma ray. Absorber was rolled foil (0.20 mg/cm^2 of Fe^{57}, natural isotopic abundance). The energy shift ΔE is given in terms of the linewidth deduced from the mean life of the state, $\Gamma=\hbar/\tau$. The dashed curves give the time spectra when the source was vibrated; the solid curves are the theoretical predictions.

expression at the end of Sec. II, the values of parameters given in Table I being used. These are all as expected except β; all theoretical curves are plotted for a value of β twice that obtained from the weight of the absorber foil. With this reservation and when allowance is made for the effect of finite resolution time, the fit between theory and experiment is fairly good. In particular, the predicted overshoot was observed; this is most noticeable in Fig. 7, where the curves for 5Γ, 7Γ, and 11Γ show that, at certain times, a higher intensity is obtained with the absorber than without it.

We have chosen to plot the relative transmission as a function of time, using the energy shift ΔE as a parameter to label the various curves. This has the advantage of allowing a direct estimate of the effect of time resolution. One could, of course, plot the transmission as a function of ΔE with the time as a parameter. This is done in Fig. 10 which shows the theoretical and experimental transmission (relative to that of the vibrated condition) vs ΔE for the times $t=\tau/2$ and $t=4\tau$ after the formation of the excited state. Note that the apparent half-width at half maximum decreases from about 3Γ at $t=\tau/2$ to about 0.7Γ at $t=4\tau$. The half-width measured without consideration of time was about 1.6Γ for this particular absorber (1.27 mg/cm^2 Fe^{57}).

In some cases the discrepancies are larger than experimental error. A number of possible sources of deviation from the theory were investigated. First, the theory assumes that no scattered radiation was detected. However, the geometric arrangement we used in order to keep the coincidence rate high was such that any appreciable scattering would have been detected. We made a crude check of this by increasing the distance from the source to detector from $\frac{3}{4}$ in. to 2 in. The fact that no change in the time spectra other than the reduced counting rate was observed indicates that scattered radiation was not contributing to the effect. Second, the source and detector might be polarized (because of permanent magnetization or by stray magnetic field) and thus change the relative intensities and polarizations of the hyperfine lines. To test for static polarization of source and detector, transmission measurements were made with various orientations of the clamped source and absorber. No effect larger than the statistical accuracy of 1% was found. In another measurement, an upper limit of 5 gauss was put on the local magnetic field, with a probable value close to the earth's field. These two observations make it unlikely that the source or absorbers were polarized. Third, because the measured linewidths were somewhat greater than they should have been, one should perhaps average over a range of energy shifts in the region of the nominal displacement ΔE. A series of curves were calculated by averaging the curves for a given ΔE over a Gaussian distribution of ΔE. Although the agreement between theory and experiment could be improved in some cases in this way, it was worse in other cases and no net improvement resulted.

TABLE I. Values of parameters used with theory of Sec. II to fit data in Figs. 6, 7, 8, and 9.

Parameter	Value	Comment
f	0.6	Fraction of 14.4-kev gamma rays emitted without recoil.
f'	0.6	Fraction of Fe^{57} nuclei absorbing without recoil.
α	15	Internal conversion coefficient.
σ_0	1.48×10^{-18} cm^2	Peak absorption cross section for no hyperfine splitting.
β	$2N\sigma_0 f'$	Thickness parameter of theory. (This value is twice the expected value.)
N	...	Number of Fe^{57} nuclei per cm^2 in absorber. (Obtained from weight of foil.)

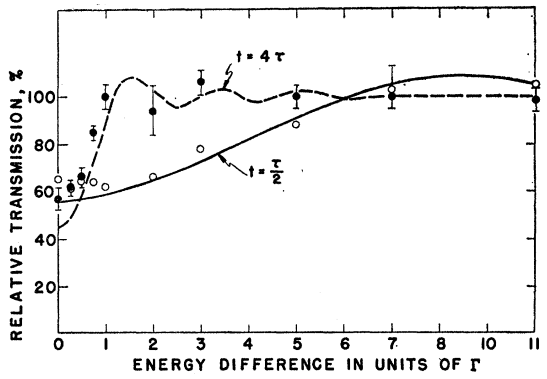

FIG. 10. Transmission (relative to the vibrated condition) of enriched Fe^{57} absorber obtained at $\frac{1}{2}\tau$ and 4τ after formation of the 14.4-kev state. The solid and dashed curves represent the theoretical predictions; the circles the experimental data points.

ACKNOWLEDGMENTS

We are indebted to Dr. G. J. Perlow and Dr. S. S. Hanna for suggesting the original problem and for supplying the proper sources and absorbers for performing the experiments. J. B. Baumgardner and A. Vandergust built most of the special electronic circuits used.

APPENDIX

The integral

$$a'(t)=\frac{1}{2\pi i}\int_{-\infty}^{+\infty}d\omega\frac{e^{i\omega t}}{\omega-\omega_0-\frac{1}{2}i\lambda}\exp\left[\frac{2ib\omega}{\omega^2-\omega_0'^2-i\omega\lambda}\right], \quad \text{(A1)}$$

can be evaluated by completing the contour on a semicircle in the upper half of the complex ω plane and finding the residues of the integrand. Since $\omega_0'\gg\lambda$, the exponent has singularities at $\omega=\pm\omega_0'+\frac{1}{2}i\lambda$. It is easily shown that the contribution from $\omega=-\omega_0'+\frac{1}{2}i\lambda$ contains a factor λ/ω_0', so this term can be neglected.

We are then left with

$$a'(t)=\frac{1}{2\pi i}\oint d\omega\frac{e^{i\omega t}}{\omega-\omega_0-\frac{1}{2}i\lambda}$$
$$\times\exp[ib(\omega-\omega_0'-\tfrac{1}{2}i\lambda)^{-1}]\equiv\frac{1}{2\pi i}\oint G d\omega$$
$$=\frac{1}{2\pi i}\left[\oint_{\omega_0+\frac{1}{2}i\lambda}G d\omega+\oint_{\omega_0'+\frac{1}{2}i\lambda}G d\omega\right]. \quad \text{(A2)}$$

In the first integral we let $z=\omega-\omega_0-\frac{1}{2}i\lambda$ so that

$$I_1=\frac{1}{2\pi i}\oint_{\omega_0+\frac{1}{2}i\lambda}G d\omega=\frac{1}{2\pi i}\exp(i\omega_0 t-\tfrac{1}{2}\lambda t)$$
$$\times\oint_{z=0}\frac{dz}{z}e^{itz}\exp[ib(z+\omega_0-\omega_0')^{-1}]$$
$$=\exp[i\omega_0 t-\tfrac{1}{2}\lambda t+ib/(\omega_0-\omega_0')]. \quad \text{(A3)}$$

In the second integral we set $z=\omega-\omega_0'-\frac{1}{2}i\lambda$ so that

$$I_2=\frac{1}{2\pi i}\oint_{\omega_0'+\frac{1}{2}i\lambda}G d\omega=\frac{1}{2\pi i}\exp[i\omega_0' t-\tfrac{1}{2}\lambda t]$$
$$\times\oint_{z=0}\frac{dz}{z+\omega_0'-\omega_0}\exp\left[i\left(tz+\frac{b}{z}\right)\right]$$
$$=-\frac{1}{2\pi i}\exp[i\omega_0' t-\tfrac{1}{2}\lambda t]$$
$$\times\oint\sum_{n=0}^{\infty}dz\frac{z^n}{(\omega_0-\omega_0')^{n+1}}\exp\left[i\left(tz+\frac{b}{z}\right)\right]. \quad \text{(A4)}$$

From the formula for generating Bessel functions,

$$\exp[\tfrac{1}{2}x(u-1/u)]=\sum_{m=-\infty}^{+\infty}u^m J_m(x), \quad \text{(A5)}$$

we find

$$\exp\left[i\left(tz+\frac{b}{z}\right)\right]=\sum_{m=-\infty}^{\infty+}i^m(t/b)^{\frac{1}{2}m}z^m J_m(2b^{\frac{1}{2}}t^{\frac{1}{2}}). \quad \text{(A5a)}$$

Substitution in Eq. (A4) yields

$$I_2=\frac{1}{2\pi i}\oint_{\omega_0'+\frac{1}{2}i\lambda}G d\omega$$
$$=-\exp[i\omega_0' t-\tfrac{1}{2}\lambda t]\sum_{n=0}^{\infty}\left(\frac{ib}{\omega_0-\omega_0'}\right)^{n+1}$$
$$\times(bt)^{-\frac{1}{2}(n+1)}J_{n+1}(2b^{\frac{1}{2}}t^{\frac{1}{2}}) \quad \text{(A6)}$$
$$=-\exp[i\omega_0' t-\tfrac{1}{2}\lambda t]\sum_{n=1}^{\infty}\left[\frac{ib}{\omega_0-\omega_0'}\right]^n$$
$$\times(bt)^{-n/2}J_n(2b^{\frac{1}{2}}t^{\frac{1}{2}}) \quad \text{(A6a)}$$
$$=-\exp[i\omega_0' t-\tfrac{1}{2}\lambda t]\left[\sum_{n=-\infty}^{\infty}S_n-\sum_{n=-\infty}^{0}S_n\right], \quad \text{(A6b)}$$

where S_n is the summand in Eq. (A6a).

We use the generating function (A5) in the first sum and find a term which cancels I_1, so we are left with

$$a'(t)=\exp[i\omega_0' t-\tfrac{1}{2}\lambda t]\sum_{n=-\infty}^{0}\left[\frac{ib}{\omega_0-\omega_0'}\right]^n$$
$$\times(bt)^{-n/2}J_n(2b^{\frac{1}{2}}t^{\frac{1}{2}})$$
$$=\exp[i\omega_0' t-\tfrac{1}{2}\lambda t]\sum_{n=0}^{\infty}\left[\frac{i(\omega_0-\omega_0')}{b}\right]^n$$
$$\times(bt)^{n/2}J_n(2b^{\frac{1}{2}}t^{\frac{1}{2}}). \quad \text{(A7)}$$

For large values of $(\omega_0-\omega_0')$ it is convenient to obtain $a'(t)$ from the sum of (A3) and (A6a). Then we have

$$a'(t)=\exp[i\omega_0' t-\tfrac{1}{2}\lambda t]\left\{-\exp i\left[\frac{b}{\omega_0-\omega_0'}+(\omega_0-\omega_0')t\right]\right.$$
$$\left.+\sum_{n=1}^{\infty}\left(\frac{ib}{\omega_0-\omega_0'}\right)^n(bt)^{-n/2}J_n(2b^{\frac{1}{2}}t^{\frac{1}{2}})\right\}. \quad \text{(A8)}$$